Available online at www.sciencedirect.com
ScienceDirect
Ceramics International 36 (2010) 1405–1409
CERAMICS INTERNATIONAL
www.elsevier.com/locate/ceramint

Low-temperature synthesis of superfine barium strontium titanate powder by the citrate method

Xiao-Fei Zhang, Qing Xu *, Yu-Heng Huang, Han-Xing Liu, Duan-Ping Huang, Feng Zhang

School of Materials Science and Engineering, Wuhan University of Technology, Wuhan 430070, People's Republic of China

Received 20 November 2009; received in revised form 7 December 2009; accepted 28 January 2010
Available online 1 March 2010

Abstract

$Ba_{0.6}Sr_{0.4}TiO_3$ powder was synthesized by a citrate method. The phase development was examined with respect to calcining temperature and heating rate during the calcining process. The results reveal a crucial role of the heating rate to the formation of a pure perovskite phase at low calcining temperatures. It was found that keeping relatively low heating rates $\leq$0.7 °C/min during the calcining process after 300 °C was favorable to a sufficient decomposition of $(Ba,Sr)_2Ti_2O_5{\cdot}CO_3$ intermediate phase at low temperatures and consequently led to the formation of a pure perovskite phase at 550 °C. $Ba_{0.6}Sr_{0.4}TiO_3$ powder calcined at the temperature under the heating rate of 0.7 °C/min showed a superfine and uniform particle morphology and high sintering reactivity. As a result, the ceramic specimens prepared from the powder attained reasonable relative densities (94–95%) at sintering temperatures of 1250–1270 °C.

Keywords: A. Calcination; A. Powders: chemical preparation; A. Sintering; D. Pervoskites

1. Introduction

In the past decades, barium strontium titanate ($(Ba,Sr)TiO_3$, BST) has drawn increasing research interest because of its strong dielectric nonlinearity under bias electric field and linearly adjustable Curie temperature with the strontium content. The desired properties make BST a promising candidate material for tunable microwave dielectric devices [1]. The applications of BST in tunable microwave devices have been explored in various forms, such as bulk ceramics, thin films and thick films [2]. BST thick films integrate the merits of lower fabrication costs compared with the thin film and smaller bias voltages required for tuning relative to the bulk ceramics. Fabricating BST thick films on alumina substrates by screen-printing or tape-casting has been believed to be cost-effective and flexible in view of mass production [3,4]. However, these thick films suffer from severe reactions with the substrates at high sintering temperatures [3,5]. Therefore, their sintering temperatures have to be limited to less than 1300 °C, which, in turn, leads to porous thick films with poor adhesion to the substrates [5]. Adding sintering aids, such as glass frits [5,6] and oxide additives [3,7], is an usually employed strategy to overcome the problem. Nevertheless, the reactions between BST thick films and the sintering aids may result in unfavorable changes in the structure and dielectric properties [6]. Thus, improving the sinterability of BST materials without adding the sintering aids appears as an intriguing subject of practical importance.

Adopting superfine starting powders with high reactivity is a viable approach to enhance the sinterability of BST materials. There have been extensive researches on preparing superfine BST powders by various chemical solution methods, such as hydrothermal synthesis [8,9], sol–gel process [10], co-precipitation route [11] and citrate precursor method [12,13]. The citrate method is essentially a polymeric precursor method, using citric acid and water as the complex agent and solvent, respectively. $(Ba,Sr)CO_3$ impurity phase usually appears together with a perovskite phase in the BST powders synthesized by the citrate method. As a result, high calcining temperatures (e.g. 800 °C) are normally required to fully eliminate the $(Ba,Sr)CO_3$ impurity phase through a solid-state reaction mechanism [14]. Previous researches have investigated the formation mechanism of BST from the citrate synthetic process [13,14]. However, how to reduce the

* Corresponding author. Tel.: +86 27 87863277; fax: +86 27 87864580.
E-mail address: xuqing@whut.edu.cn (Q. Xu).

0272-8842/$36.00
doi:10.1016/j.ceramint.2010.02.004

formation temperature of BST with a pure perovskite phase remains as an issue to be resolved. It is expected that synthesizing BST at lower temperatures would lead to an easy morphology control and improved sinterability for the resulting powders.

In this work, we report low-temperature synthesis of $Ba_{0.6}Sr_{0.4}TiO_3$ powder via the citrate method by deliberately controlling heating rate of the calcining process. Moreover, the sinterability of the resulting powder was examined.

2. Experimental

$Ba_{0.6}Sr_{0.4}TiO_3$ powder was synthesized by the citrate method. Reagent grade $Ba(NO_3)_2$, $Sr(NO_3)_2$, tetrabutyl titanate and citrate acid were used as starting materials. Citric acid was dissolved in deionized water in a beaker. Aqueous ammonia was dripped to adjust the pH value of the solution to 7–9. Then tetrabutyl titanate was slowly added under a stirring at 70 °C to form a transparent aqueous solution. Various nitrates were added according to the nominal composition. The mole ratio of citric acid to the total metal cation content was 1.5. After stirring at 80 °C for 1 h, a transparent precursor solution with a pH value of about 6 was yielded. The precursor solution was subjected to heating in an oven at 300 °C to form a foam-like solid precursor. The foam precursor was pulverized and calcined at different temperatures under heating rates of 0.7–1.1 °C/min during the calcining process after 300 °C in air. The calcined powders were uniaxially pressed into discs under a pressure of 300 MPa and subsequently sintered at 1200–1300 °C for 2 h in air.

Thermogravimetry (TG) and differential scanning calorimetry (DSC) analysis of the foam precursor were performed by a Netzsch STA 449C simultaneous thermal analyzer at a heating rate of 5 °C/min in air. The phase purity of the calcined powders was examined by a Philips X'pert PBO X-ray diffractometer using Cu Kα radiation. The morphology of the calcined powders was observed at a Jeol JSM-5610LV scanning electron microscope (SEM) and a Hitachi S-4700 field emission scanning electron microscope (FESEM), respectively. The dilatometric measurement of the compacted powders was conducted by a Netzsch DIL 402C dilatometer at a heating rate of 5 °C/min between 20 and 1300 °C in air. The bulk densities of the ceramic specimens were measured by the Archimedes method with ethyl alcohol as the medium. The relative densities were determined from the measured data and X-ray theoretical density of $Ba_{0.6}Sr_{0.4}TiO_3$.

3. Results and discussion

Fig. 1 shows the TG–DSC curves of the foam precursor. A weak endothermic peak could be found at around 90 °C, accompanied by a small weight loss of 4.8%. This change is ascribed to the evaporation of absorbed water. A sharp exothermic peak occurred at around 450 °C, corresponding to a large weight loss of 37.7%. This occurrence can be attributed to the decomposition and burning of residual carbon components. No further DSC peak or weight loss could be seen after 620 °C. This result indicates that the decomposition of the precursor was finished before the temperature.

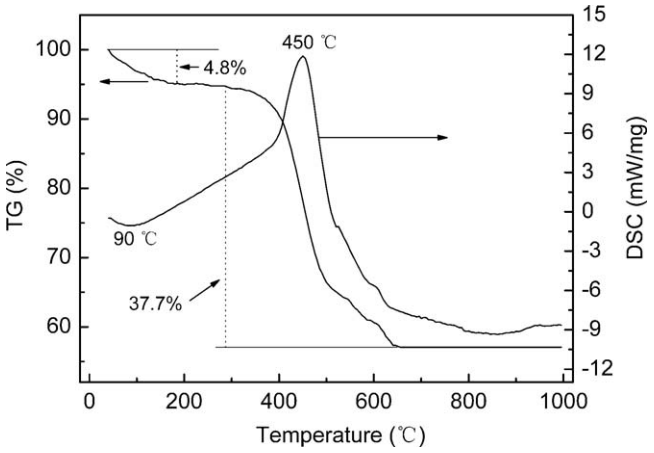

Fig. 1. TG–DSC curves of the foam-like precursor.

Fig. 2 shows the X-ray diffraction (XRD) patterns of $Ba_{0.6}Sr_{0.4}TiO_3$ powders calcined at different temperatures under a heating rate of 0.7 °C/min during the calcining process after 300 °C. The foam-like precursor showed an amorphous nature. A diffuse XRD peak appeared after calcining at 400 °C, which can be assigned to an intermediate phase $(Ba,Sr)_2Ti_2O_5{\cdot}CO_3$ (BSTOC) [13,15]. A perovskite phase was formed together with the BSTOC intermediate phase at 500 °C. Further elevating the calcining temperatures to 550 and 600 °C, respectively, produced a pure $Ba_{0.6}Sr_{0.4}TiO_3$ phase. These results suggest that the BSTOC intermediate phase appeared prior to the $Ba_{0.6}Sr_{0.4}TiO_3$ perovskite phase, with the perovskite phase being derived from the decomposition of the intermediate phase. This suggestion is consistent with previous result regarding the synthesis of BST from the citrate precursor [13].

Fig. 3 shows the XRD patterns of $Ba_{0.6}Sr_{0.4}TiO_3$ powders calcined at different temperatures under a heating rate of 0.9 °C/min during the calcining process after 300 °C. Compared with Fig. 2, the relatively higher heating rate resulted in a different phase development for the calcined powders. The BSTOC intermediate phase was detected together with a $(Ba,Sr)CO_3$

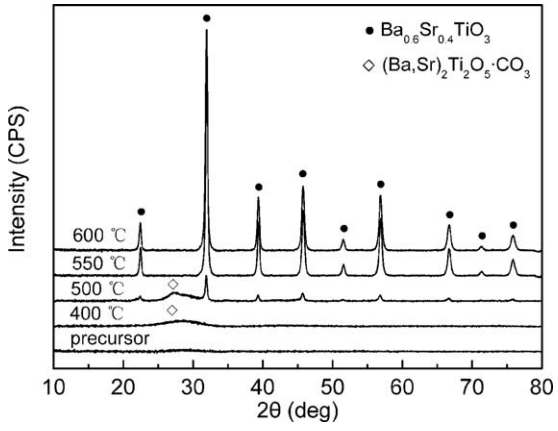

Fig. 2. XRD patterns of $Ba_{0.6}Sr_{0.4}TiO_3$ powders calcined at different temperatures under the heating rate of 0.7 °C/min.

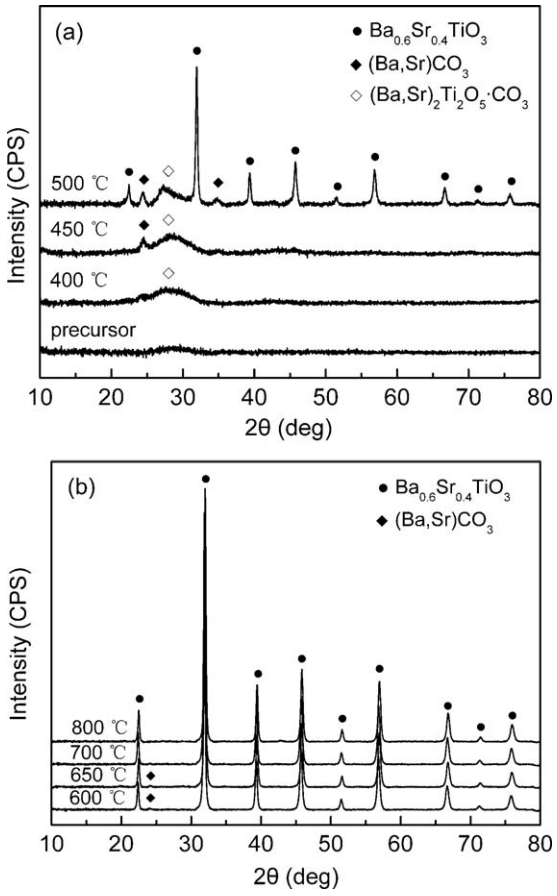

Fig. 3. XRD patterns of $Ba_{0.6}Sr_{0.4}TiO_3$ powders calcined at different temperatures under the heating rate of 0.9 °C/min.

(BSC) phase when calcining at 450 °C. The BSTOC intermediate phase disappeared after calcining at 600 °C, while a tiny amount of the BSC phase still remained at 650 °C. A pure perovskite phase was finally produced at 700 °C. The comparison of Figs. 2 and 3 indicates a sensitivity of phase development to the heating rate for the calcined powders.

Fig. 4 shows the XRD patterns of $Ba_{0.6}Sr_{0.4}TiO_3$ powders calcined at 550 °C under different heating rates during the calcining process after 300 °C. A pure perovskite phase was identified for the powders calcined at the heating rates of 0.5 and 0.7 °C/min, respectively, whereas the higher heating rates (0.9 and 1.1 °C/min) led to the existence of the BSTOC and BSC phases together with a perovskite phase. As to the powders calcined at the higher heating rates (0.9 and 1.1 °C/min), the intensity of the XRD peak corresponding to the BSC phase tended to increase with the heating rate. These results further substantiate the sensitivity of phase development to the heating rate for the calcined powders.

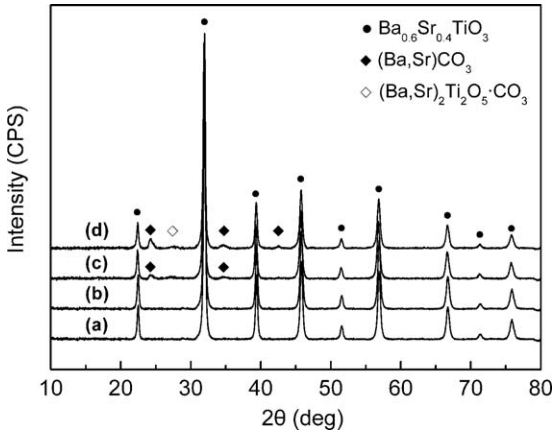

Fig. 4. XRD patterns of $Ba_{0.6}Sr_{0.4}TiO_3$ powders calcined at 550 °C under the heating rates of (a) 0.5 °C/min, (b) 0.7 °C/min, (c) 0.9 °C/min and (d) 1.1 °C/min.

The distinct phase developments of the calcined powders at different heating rates can be tentatively explained with respect to the formation mechanism of BST from the citrate precursor. It has been reported that the formation of BST at low temperatures can be realized via a thermal decomposition of the intermediate phase BSTOC, as described by the following equation [13,15]:

$$(Ba,Sr)_2Ti_2O_5{\cdot}CO_3 \rightarrow 2(Ba,Sr)TiO_3 + CO_2 \quad (1)$$

The XRD inspection of the present work (Figs. 1–3) indicates that the decomposition reaction occurred between 500 and 550 °C. This reaction temperature range is generally consistent with the literature result [13]. On the other hand, the thermal decomposition of the BSTOC intermediate phase can proceed via an alternative route:

$$(Ba,Sr)_2Ti_2O_5{\cdot}CO_3 + CO_2 \rightarrow 2(Ba,Sr)CO_3 + 2TiO_2 \quad (2)$$

The carbon dioxide presumably originated from the burning of residual carbon components. The presence of the BSC phase in the calcined powders (Figs. 3 and 4) can be viewed as an evidence for the occurrence of the reaction. The absence of XRD peaks corresponding to TiO_2 is presumed to be due to its amorphous nature [13,14]. Thus, the phase development of the calcined powders appears to be dependent on the competition of the two reaction mechanisms. Similar phenomenon has been found in the synthesis of $BaTiO_3$ by the citrate method. It has been reported that the onset formation temperature of $BaTiO_3$ from the decomposition of an intermediate phase $Ba_2Ti_2O_5{\cdot}CO_3$ was about 550 °C, while the decomposition of the intermediate phase into $BaCO_3$ happened at 600–650 °C [16]. We believe that the reaction sequence can be applied to the present work on account of an analogous material nature and an essentially identical synthetic principle. That is, the reaction described by Eq. (2) occurred at relatively higher temperatures compared with that depicted by Eq. (1).

On this ground, the sensitivity of phase development to the heating rate is conceivable. A slow heating rate permits a sufficient decomposition of the BSTOC intermediate phase at relatively low temperatures according to Eq. (1) and, as a result, avoids the generation of the BSC phase at relatively high temperatures. On the contrary, a fast heating rate is unfavorable to this occurrence, leading to the formation of the BSC phase. Moreover, a fast heating rate is prone to induce intense combustion of residual carbon components during the calcination (Fig. 1) and consequently cause local high temperature. The appearance of the BSC phase after calcining at 450 °C in Fig. 3 can be visualized as a consequence of intense combustion and the resulting local high temperature caused by the comparatively fast heating rate.

The formed BSC impurity phase was eliminated at temperatures higher than 600 °C through a solid-state reaction with the amorphous TiO_2 [13]:

$$(Ba, Sr)CO_3 + TiO_2 \rightarrow (Ba, Sr)TiO_3 + CO_2 \quad (3)$$

In the present work, the calcined temperature required for eliminating the impurity phase was 700 °C, which is lower than the literature results (750–800 °C) [14,17]. This discrepancy may be attributed to different reactivities of formed BSC depending on synthetic procedures.

From above discussion, one can argue that the heating rate plays an important role in determining the dynamics of the thermal decomposition of the intermediate phase and, consequently, the phase development of the calcined powders. The present result manifests that appropriately controlling the heating rate allows for producing $Ba_{0.6}Sr_{0.4}TiO_3$ powder with a pure perovskite phase at 550 °C. This formation temperature is lowered by about 250 °C compared with the literature results regarding synthesizing BST powders by the citrate method [12–14]. In addition, the BSC is an often-detected impurity phase in BST powders derived from various hydrocarbon precursors [17–19]. The results of the present work might serve to be a clue to modify the synthesis of BST powders by using these chemical methods.

The morphology of $Ba_{0.6}Sr_{0.4}TiO_3$ powder calcined at 550 °C under the heating rate of 0.7 °C/min was investigated by SEM and FESEM techniques, respectively, as shown in Fig. 5. The SEM image (Fig. 5a) offered a panoramic view of the powder morphology, showing fine and uniform particles. The FESEM image (Fig. 5b) further revealed that the size of preliminary particles was 20–30 nm and there exist spongy agglomerations (around 100 nm) of the preliminary particles. The BET measurement indicated a specific surface area of 19.0 m^2/g for the powder. The mean particle size was estimated to be 55.6 nm based on the specific surface area, which generally agrees with the FESEM observation. These results confirm a fine and uniform morphology for the $Ba_{0.6}Sr_{0.4}TiO_3$ powder.

Fig. 6 shows the dilatometric curves of the pressed specimen prepared from the $Ba_{0.6}Sr_{0.4}TiO_3$ powder. The specimen started to shrink at 1066 °C, attained a maximum shrinkage rate at 1218 °C and displayed a rapid decrease of shrinkage rate at the higher temperatures. A small shoulder appeared at the shrinkage curve at around 1300 °C, corresponding to an abrupt change of the shrinkage rate. This anomaly is believed to be caused by the creation of eutectic liquid phase [20]. The dilatometric analysis implies relatively lower densification temperatures for the powder.

Fig. 7 shows the relative density as function of sintering temperature for the ceramic specimens prepared from the $Ba_{0.6}Sr_{0.4}TiO_3$ powder. The specimens displayed a densification increment with sintering temperature within 1200–1270 °C. Sintering at the higher temperatures resulted in a decline of the relative density. This densification decrement can be explained with the generation of eutectic liquid phase. It has been reported eutectic liquid phase generated in the barium strontium titanate system at high temperatures during sintering [20]. The small shoulder in the shrinkage curve at about

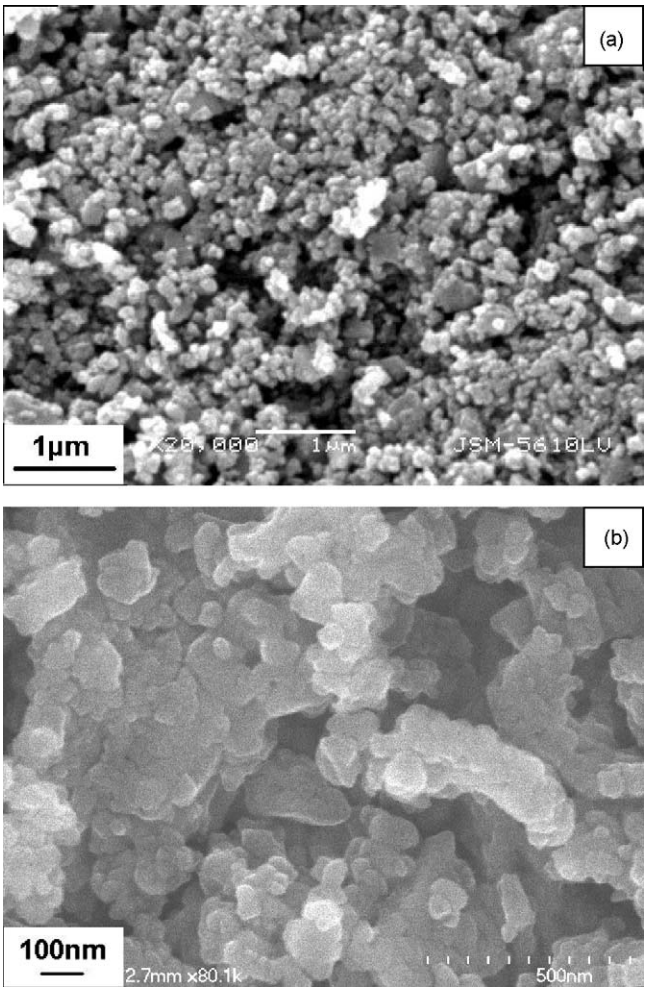

Fig. 5. (a) SEM and (b) FESEM images of $Ba_{0.6}Sr_{0.4}TiO_3$ powder calcined at 550 °C under the heating rate of 0.7 °C/min.

1300 °C (see Fig. 6) can be regarded as an indication of sharp increase of the liquid phase amount around the temperature. The liquid phase has a nonwetting nature, which is unfavorable to the densification of the specimens [21]. This effect is assumed to be responsible for the decline in relative density for the specimens sintered at 1280–1300 °C.

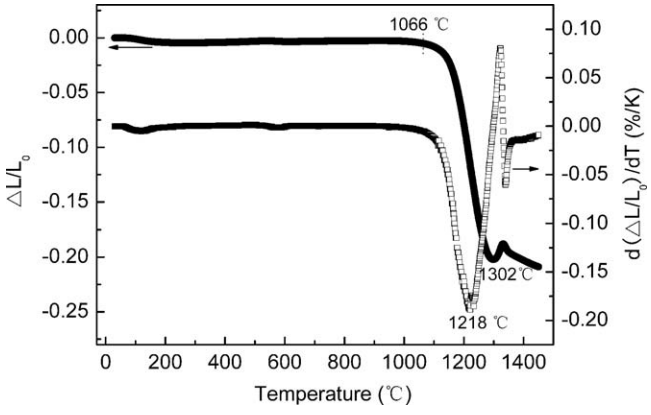

Fig. 6. Dilatometric curves of the compressed specimen prepared from $Ba_{0.6}Sr_{0.4}TiO_3$ powder calcined at 550 °C under the heating rate of 0.7 °C/min.

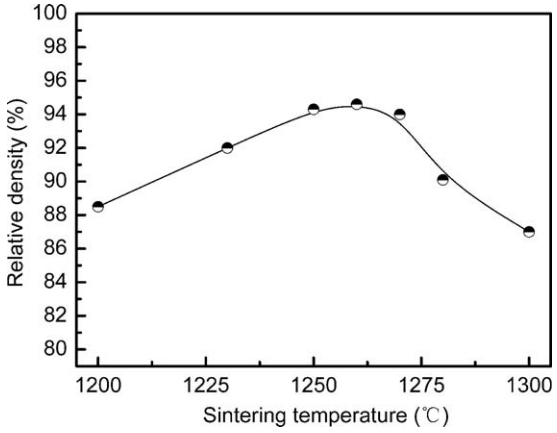

Fig. 7. Relative density as function of sintering temperature for the ceramic specimens prepared from $Ba_{0.6}Sr_{0.4}TiO_3$ powder calcined at 550 °C under the heating rate of 0.7 °C/min.

The ceramic specimens attained reasonable relative densities of 94–95% at 1250–1270 °C. These relative densities are roughly comparable with those of BST ceramics prepared by the conventional solid-state reaction method and sintered at 1400 °C or higher temperatures [3,20,22]. The sintering temperatures of the specimens (1250–1270 °C) required for achieving reasonable densification are comparatively lower than those (1320–1350 °C) of BST ceramics prepared by other chemical methods [23,24]. These comparisons demonstrate a high sintering reactivity of the powder derived from the citrate method at the low calcining temperature, which can be attributed to its fine and uniform morphology.

4. Conclusions

$Ba_{0.6}Sr_{0.4}TiO_3$ powders have been synthesized by the citrate method under different heating rates during the calcining process after 300 °C. The heating rate was found to be vital to the phase development of the powders. Appropriately controlling the heating rate allowed for synthesizing $Ba_{0.6}Sr_{0.4}TiO_3$ powders with a pure perovskite phase at 550 °C. $Ba_{0.6}Sr_{0.4}TiO_3$ powder calcined at the temperature under the heating rate of 0.7 °C/min showed a desired morphology and an improved sinterability. The ceramic specimens prepared from the powder attained 94–95% of the theoretic density after sintering at 1250–1270 °C.

Acknowledgements

This work was supported by the Ministry of Education (No. 108092), National Natural Science Foundation of China (No. 50932004 and A3 Foresight Program-50821140308) and Wuhan Science and Technology Bureau (No. 200851430485).

References

[1] L.C. Sengupta, S. Sengupta, Breakthrough advances in low loss, tunable dielectric materials, Mater. Res. Innov. 2 (1999) 278–282.
[2] A.K. Tagantsev, V.O. Sherman, K.F. Astafiev, J. Venkatesh, N. Setter, Ferroelectric materials for microwave tunable applications, J. Electroceram. 11 (2003) 5–66.
[3] B. Su, T.W. Button, Interactions between barium strontium titanate (BST) thick films and alumina substrates, J. Eur. Ceram. Soc. 21 (2001) 2777–2781.
[4] B. Su, J.E. Holmes, C. Meggs, T.W. Button, Dielectric and microwave properties of barium strontium titanate (BST) thick films on alumina substrates, J. Eur. Ceram. Soc. 23 (2003) 2699–2703.
[5] D. Zhang, W.F. Hu, C. Meggs, B. Su, T. Price, D. Iddles, M.J. Lancaster, T.W. Button, Fabrication and characterisation of barium strontium titanate thick film device structures for microwave applications, J. Eur. Ceram. Soc. 27 (2007) 1047–1051.
[6] R. Wu, P.Y. Du, W.J. Weng, G.R. Han, Preparations and dielectric properties of $Ba_{0.80}Sr_{0.20}TiO_3/PbO–B_2O_3$ thick films, Mater. Chem. Phys. 97 (2006) 151–155.
[7] T. Tick, J. Perantie, H. Jantunen, A. Unsimaki, Screen printed low-sintering-temperature barium strontium titanate (BST) thick films, J. Eur. Ceram. Soc. 28 (2008) 837–842.
[8] R.K. Roeder, E.B. Slamovich, Stoichiometry control and phase selection in hydrothermally derived $Ba_xSr_{1-x}TiO_3$ powders, J. Am. Ceram. Soc. 82 (1999) 1665–1675.
[9] B.L. Gersten, M.M. Lencka, R.E. Riman, Low-temperature hydrothermal synthesis of phase-pure (Ba,Sr)TiO_3 perovskite using EDTA, J. Am. Ceram. Soc. 87 (2004) 2025–2032.
[10] P.K. Sharma, V.V. Varadan, V.K. Varadan, Porous behavior and dielectric properties of barium strontium titanate synthesized by sol–gel method in the presence of triethanolamine, Chem. Mater. 12 (2000) 2590–2596.
[11] Y.B. Khollam, S.V. Bhoraskar, S.B. Deshpande, H.S. Potdar, N.R. Pavaskar, S.R. Sainkar, S.K. Date, Simple chemical route for the quantitative precipitation of barium–strontium titanyl oxalate precursor leading to $Ba_{1-x}Sr_xTiO_3$ powders, Mater. Lett. 57 (2003) 1871–1879.
[12] C. Shen, Q.F. Liu, Q. Liu, Sol–gel synthesis and spark plasma sintering of $Ba_{0.5}Sr_{0.5}TiO_3$, Mater. Lett. 58 (2004) 2302–2305.
[13] C.L. Mao, X.L. Dong, T. Zeng, G.H. Wang, S. Shen, Formation and control of mechanism for the preparation of ultra-fine barium strontium titanate powders by the citrate precursor method, Mater. Res. Bull. 42 (2007) 1602–1610.
[14] C.L. Mao, X.L. Dong, T. Zeng, Synthesis and characterization of nanocrystalline barium strontium titanate powders prepared by citrate precursor method, Mater. Lett. 61 (2007) 1633–1636.
[15] S.Y. Chen, H.W. Wang, L.C. Huang, Role of an intermediate phase $(Ba,Sr)_2Ti_2O_5·CO_3$ in doped $(Ba_{0.7}Sr_{0.3})TiO_3$ thin films, Mater. Chem. Phys. 77 (2002) 632–638.
[16] P. Duran, F. Capel, D. Gutierrez, J. Tartaj, M.A. Banares, C. Moure, Metal citrate polymerized complex thermal decomposition leading to the synthesis of $BaTiO_3$: effects of the precursor structure on the $BaTiO_3$ formation mechanism, J. Mater. Chem. 11 (2001) 1828–1836.
[17] J.Q. Huang, M.C. Hong, F.L. Jiang, Y.G. Cao, Synthesis of nanosized perovskite (Ba,Sr)TiO_3 powder via a PVA modified sol-precipitation process, Mater. Lett. 62 (2008) 2304–2306.
[18] J.W. Zhai, X. Yao, X.G. Cheng, L.Y. Zhang, H. Chen, Dielectric properties under dc-bias field of $Ba_{0.6}Sr_{0.4}TiO_3$ with various grain sizes, Mater. Sci. Eng. B 94 (2002) 164–169.
[19] A. Ries, A.Z. Simoes, M. Cilense, M.A. Zaghete, J.A. Varela, Barium strontium titanate powder obtained by polymeric precursor method, Mater. Charact. 50 (2003) 217–221.
[20] B. Su, J.E. Holmes, B.L. Chen, T.W. Button, Processing effects on the microstructure and dielectric properties of barium strontium titanate (BST) ceramics, J. Electroceram. 9 (2002) 111–116.
[21] B. Su, T.W. Button, Microstructure and dielectric properties of Mg-doped barium strontium titanate ceramics, J. Appl. Phys. 95 (2004) 1382–1385.
[22] X.F. Liang, Z.Y. Meng, W.B. Wu, Effect of acceptor and donor dopants on the dielectric and tunable properties of barium strontium titanate, J. Am. Ceram. Soc. 87 (2004) 2218–2222.
[23] Q.X. Liu, X.G. Tang, Y.Y. Deng, J. Wang, H.L.W. Chan, Mater. Nonlinear dielectric properties of sol–gel derived (Ba,Sr)TiO_3 ceramics, Mater. Chem. Phys. 112 (2008) 281–284.
[24] A. Ianculescu, D. Berger, M. Viviani, C.E. Ciomaga, L. Mitoseriu, E. Vasile, N. Dragan, D. Crisan, Investigation of $Ba_{1-x}Sr_xTiO_3$ ceramics prepared from powders synthesized by the modified Pechini route, J. Eur. Ceram. Soc. 27 (2007) 3655–3658.